

Rothamsted Repository Download

A - Papers appearing in refereed journals

Child, H. T., Deeks, M. J., Haynes, K., Rudd, J. J. and Bates, S. 2022. Distinct roles for different autophagy-associated genes in the virulence of the fungal wheat pathogen *Zymoseptoria tritici*. *Fungal Genetics and Biology*. 163, p. 103748. <https://doi.org/10.1016/j.fgb.2022.103748>

The publisher's version can be accessed at:

- <https://doi.org/10.1016/j.fgb.2022.103748>
- https://www.sciencedirect.com/science/article/pii/S1087184522000937?utm_campaign=STMJ_AUTH_SERV_PUBLISHED&utm_medium=email&utm_acid=72188367&SIS_ID=&dgcid=STMJ_AUTH_SERV_PUBLISHED&CMX_ID=&utm_in=DM311474&utm_source=AC

The output can be accessed at: <https://repository.rothamsted.ac.uk/item/98q68/distinct-roles-for-different-autophagy-associated-genes-in-the-virulence-of-the-fungal-wheat-pathogen-zymoseptoria-tritici>.

© 26 October 2022, Please contact library@rothamsted.ac.uk for copyright queries.



Distinct roles for different autophagy-associated genes in the virulence of the fungal wheat pathogen *Zymoseptoria tritici*

Harry T. Child^a, Michael J. Deeks^a, Ken Haynes^{a,1}, Jason J. Rudd^b, Steven Bates^{a,*}

^a University of Exeter, College of Life and Environmental Sciences, Geoffrey Pope Building, Stocker Road, Exeter EX4 4QD, UK

^b Dept of Bio-Interactions and Crop Protection, Rothamsted Research, Harpenden AL5 2JQ, UK

ARTICLE INFO

Keywords:

Zymoseptoria tritici
Wheat
Autophagy
Virulence
Plant pathogen

ABSTRACT

The fungal wheat pathogen *Zymoseptoria tritici* causes major crop losses as the causal agent of the disease Septoria tritici blotch. The infection cycle of *Z. tritici* displays two distinct phases, beginning with an extended symptomless phase of 1–2 weeks, before the fungus induces host cell death and tissue collapse in the leaf. Recent evidence suggests that the fungus uses little host-derived nutrition during asymptomatic colonisation, raising questions as to the sources of energy required for this initial growth phase. Autophagy is crucial for the pathogenicity of other fungal plant pathogens through its roles in supporting cellular differentiation and growth under starvation. Here we characterised the contributions of the autophagy genes *ZtATG1* and *ZtATG8* to the development and virulence of *Z. tritici*. Deletion of *ZtATG1* led to inhibition of autophagy but had no impact on starvation-induced hyphal differentiation or virulence, suggesting that autophagy is not required for *Z. tritici* pathogenicity. Contrastingly, *ZtATG8* deletion delayed the transition to necrotrophic growth, despite having no influence on filamentous growth under starvation, pointing to an autophagy-independent role of *ZtATG8* during *Z. tritici* infection. To our knowledge, this study represents the first to find autophagy not to contribute to the virulence of a fungal plant pathogen, and reveals novel roles for different autophagy-associated proteins in *Z. tritici*.

1. Introduction

Autophagy is the process by which eukaryotic cells sequester cytoplasmic contents for degradation in the vacuole, enabling them to recycle the constituent macromolecular parts (Klionsky et al., 2011). This includes the breakdown of cytosolic proteins, organelles and intracellular pathogens (Feng et al., 2014; Orvedahl & Levine, 2009). This process plays a crucial role in cellular homeostasis under favourable conditions, through degradation of defective proteins and organelles, and in response to abiotic and biotic stress, most notably during nutrient starvation (Mizushima & Komatsu, 2011). Furthermore, autophagy functions in the extensive remodelling of cellular architecture during differentiation and tissue development (Mizushima & Levine, 2010). As well as these pro-survival and developmental roles, autophagy has been found to play diverse roles in programmed cell death across eukaryotes (Minina et al., 2014; Shimizu et al., 2004).

Macroautophagy (hereby referred to as autophagy) involves the localisation of autophagy proteins at the pre-autophagosomal structure

(PAS) adjacent to the vacuole, which initiate formation of a double membrane structure called a phagophore (Xie & Klionsky, 2007). The phagophore engulfs organelles and other cytosolic contents to form the autophagosome. The autophagosome then fuses with the vacuole, where its cargo is degraded and the resulting macromolecules transported back to the cytoplasm (Reggiori & Klionsky, 2013). This process can either be utilised for unselective sequestration of bulk cytoplasm, or the selective degradation of cytosolic proteins, via the cytoplasm to vacuole targeting (Cvt) pathway (Lynch-Day & Klionsky, 2010), and organelles.

A suite of 42 ATG (Autophagy-related Genes) genes have been found to be involved in these processes in *Saccharomyces cerevisiae* and other yeast species (Parzych et al., 2018), many of which are conserved in filamentous fungi (Kershaw & Talbot, 2009; Liu et al., 2017; Lv et al., 2017). These encode the core protein machinery required for autophagy, along with pathway specific proteins required for selective autophagy. This includes the protein kinase ATG1, which is essential for the initiation of autophagy through recruitment of ATG proteins to the PAS and phosphorylation of proteins required for autophagosome formation

* Corresponding author.

E-mail address: S.Bates@exeter.ac.uk (S. Bates).

¹ Died 19th March 2018.

(Mizushima, 2010), performing the most upstream step of autophagosome formation (Suzuki et al., 2007). Another crucial component of the autophagy machinery is the ubiquitin-like protein ATG8, which is conjugated to the autophagosome via the membrane lipid phosphatidylethanolamine (PE; Ichimura et al., 2000). Here it acts as a binding platform for other autophagy proteins and facilitates membrane tethering and hemifusion, by which it is essential for autophagosome expansion (Nakatogawa et al., 2007; Nakatogawa et al., 2012).

Despite the use of model yeast species in most research into the molecular machinery of fungal autophagy, the role of autophagy in the development of filamentous fungi has been recently investigated (Khan et al., 2012; Pollack et al., 2009). As in *S. cerevisiae*, autophagy has been shown to be vital for growth under nutrient starvation conditions in many ascomycetes (Josefsen et al., 2012; Nitsche et al., 2013; Richie et al., 2007; Shoji et al., 2010; Voigt & Pöggeler, 2013). In the mycelium of *Aspergillus oryzae*, degradation of organelles through autophagy in basal hyphal compartments is proposed to enable recycling of nutrients to the growing hyphal tips via tubular vacuoles (Shoji et al., 2006, 2010). Furthermore, autophagy supports developmental transitions between morphological forms in filamentous ascomycetes including differentiation of aerial hyphae (Liu et al., 2007; Nguyen et al., 2011; Pinan-Lucarré et al., 2005), spore germination (Liu et al., 2007), conidiation (Liu et al., 2007; Lv et al., 2017) and development of sexual fruiting bodies (Liu et al., 2007; Lv et al., 2017; Pinan-Lucarré et al., 2005).

Autophagy also plays a crucial role in the virulence of economically important fungal plant pathogens, often through involvement in cellular differentiation. Autophagy is required for host colonisation in multiple plant pathogens through its involvement in the differentiation of penetration structures termed appressoria (Asakura et al., 2009; Liu et al., 2007; Ren et al., 2017). Disruption of autophagy in the rice pathogen *Magnaporthe oryzae* causes loss of pathogenicity, due to the impairment of developmentally-regulated cell death in the conidia and an inability to build sufficient turgor pressure in the appressorium for host penetration (Kershaw & Talbot, 2009; Liu et al., 2007). Furthermore, *Fusarium graminearum* was found to require autophagy to spread between spikelets during infection of wheat (Josefsen et al., 2012). Authors suggested this was caused by the inability of autophagy-deficient mutants to utilise stored carbon to cross the nutrient-limited rachis (Josefsen et al., 2012; Nguyen et al., 2011). Autophagy was also found to support asexual and sexual reproduction in *M. oryzae* and *F. graminearum*, with autophagy mutants in both species displaying reduced conidiation and an inability to generate perithecia (Liu et al., 2007; Lv et al., 2017).

Zymoseptoria tritici is a devastating foliar pathogen of wheat, causing significant yield losses despite the deployment of genetic resistance and widespread fungicide application (Fones & Gurr, 2015; Torriani et al., 2015). *Z. tritici* exhibits an asymptomatic phase of 1–2 weeks after the spore germinates on the leaf surface, penetrating the stomata and colonising the intercellular space of the mesophyll (Kema et al., 1996). This is followed by a switch to necrotrophic growth as the fungus induces host cell death and lysis, releasing nutrients which it uses to grow rapidly and develop asexual fruiting bodies termed pycnidia (Keon et al., 2007). Initially, the early asymptomatic phase was classified as biotrophic (involving feeding on living host cells), but evidence from transcriptomic and metabolomic analysis has suggested that *Z. tritici* utilises little host-derived nutrition at this stage (Keon et al., 2007; Rudd et al., 2015), leading to the proposed definition as a “latent necrotroph” (Sánchez-Vallet et al., 2015).

Although *Z. tritici* does not form appressoria to penetrate the leaf cuticle, the transition to hyphal growth required for host colonisation involves significant changes in cellular morphology. The morphological switch and subsequent invasive growth are proposed to require recycling of stored lipids in response to the nutrient-limiting conditions on the leaf surface (Rudd et al., 2015). *Z. tritici* spores are densely packed with lipid droplets (LDs), which are less abundant in hyphal filaments

(Francisco et al., 2019; Sidhu, 2015), while transcriptome data has identified the upregulation of genes involved in lipid metabolism during early infection (Rudd et al., 2015). Autophagy has been shown to be involved in LD breakdown under starvation conditions in mammalian, yeast and filamentous fungal cells (Josefsen et al., 2012; Singh et al., 2009; van Zutphen et al., 2014).

Considering the involvement of autophagy in the growth of other ascomycete fungi under starvation stress (Liu et al., 2007; Shoji et al., 2010), and its widespread importance in virulence, we investigated the role of autophagy in *Z. tritici* development and infection. We first performed a series of homology searches for autophagy genes within the *Z. tritici* genome to produce a predicted network of *Z. tritici* autophagy components. We then performed a functional characterisation of *ZtATG1* and *ZtATG8* through targeted gene deletion. Autophagy was inhibited by deletion of *ZtATG1*, but this gene was found to be dispensable for hyphal growth under starvation and pathogenicity of *Z. tritici*. However, deletion of *ZtATG8* led to a delay in the necrotrophic switch, indicating an autophagy-independent role of *ZtATG8* during *Z. tritici* infection.

2. Materials and methods

2.1. BLAST searches and alignments

Homologs of previously characterised autophagy proteins from *S. cerevisiae* were identified in the *Z. tritici* genome through BLASTp searches against the JGI genome annotation (<https://mycocosm.jgi.doe.gov/Mycogr3/Mycogr3.home.html>) on the Ensembl Fungi *Zymoseptoria tritici* genome database (http://fungi.ensembl.org/Zymoseptoria_tritici/Tools/Blast), using default parameters apart from adjustment of the E-value threshold to 1e-3. Upon failure to identify a hit, tBLASTn searches were carried out against the genome sequence to identify homologous gene models from the recent Rothamsted Research (RRes; King et al., 2017) and Max Planck Institute (MPI) annotations. Additionally, BLAST searches for pexophagy-specific proteins from *Pichia pastoris* (ATG28, ATG30, ATG35, ATG37) and *Pichia angustata* (ATG25) were carried out. Where no *Z. tritici* homologs were identified, ATG protein sequences from *M. oryzae* were used in BLAST searches, as the closest filamentous ascomycete relative of *Z. tritici* in which autophagy has been extensively characterised (Kershaw & Talbot, 2009). Pairwise protein alignments were carried out with predicted *S. cerevisiae* and *M. oryzae* ATG proteins as query sequences, to assess sequence identity across the whole protein. Multiple sequence alignments were carried out using the M-Coffee program (Di Tommaso et al., 2011).

2.2. Microbial strains and growth conditions

The reference *Z. tritici* strain IPO323 was used in this study (Goodwin et al., 2011). *Z. tritici* blastospores were routinely cultured on YPD agar at 19 °C under darkness for 5 days before use in transformations and phenotypic assays. Other microbial strains and growth conditions are described in Sidhu et al. (2015).

2.3. Construction of targeted gene deletion and GFP-fusion vectors

Construction of plasmid vectors for the deletion of *ZtATG1* and *ZtATG8* was carried out by yeast recombinational cloning, following the previously described method (Sidhu et al., 2015). The plasmid pC-HYG-YR was used as a backbone for these vectors (Sidhu et al., 2015). Left flank (LF) and right flank (RF) sequences were PCR amplified using the primer pairs *ZtATG1*-LF-F/R, *ZtATG1*-RF-F/R, *ZtATG8*-LF-F/R and *ZtATG8*-RF-F/R (Table S1). LF and RF amplicons were transformed into *S. cerevisiae* alongside the pC-HYG-YR vector, which had been linearised by restriction digestion with the enzymes EcoRI and HindIII (New England Biolabs, UK). This resulted in the plasmids pC-HYG-ATG1KO and pC-HYG-ATG8KO.

The plasmid pC-SUR-GFPATG8 was also generated for expression of a ZtGFP:ZtATG8 fusion protein from the wild type ZtATG8 locus. This was constructed using the *Z. tritici* codon-optimised GFP (Kilaru et al., 2015). The ZtATG8 LF sequence, which includes the pZtATG8 native promoter, was amplified with the primers ZtATG8_LF_F and ZtATG8_LF_GFP_R containing 5' primer extensions overlapping the left border sequence and start of ZtGFP, respectively (Table S1). The ZtATG8 open reading frame and terminator were amplified with primers ZtATG8_GFP_F and ZtATG8_R containing 5' extensions overlapping the end of ZtGFP (with the stop codon replaced by a tri-alanine linker) and the start of the SUR^R selection cassette, respectively (Table S1). A right flank sequence (RF2) starting downstream of the ZtATG8 terminator was amplified with the primers ZtATG8-RF2-F/R containing 5' extensions overlapping the end of the SUR^R cassette and the right border sequence, respectively. Finally, the ZtGFP coding sequence lacking a stop codon was amplified with the primers ZtGFP_F and ZtGFP_NOSTOP_R (Table S1). These fragments were transformed into *S. cerevisiae* with the linearised pC-SUR-YR plasmid to form the plasmid pC-SUR-GFPATG8. Constructed plasmids were extracted from *S. cerevisiae*, amplified in *E. coli* and screened for fidelity of PCR amplification by Sanger sequencing.

2.4. *Agrobacterium tumefaciens*-mediated transformation of *Z. tritici*

Plasmid vectors were transformed into *Z. tritici* by *A. tumefaciens*-mediated transformation (ATMT), using the protocol deposited on protocols.io (Child & Helmstetter, 2022) which describes modifications of the original protocol (Zwiers & de Waard, 2001).

2.5. FM4-64 staining

Z. tritici spores were harvested after growth on YPD agar plates for 5 days and suspended in 1 ml yeast extract glucose (YG) broth containing 16 µM FM4-64 stain (Sigma-Aldrich, UK). Spore suspensions were incubated at 19 °C for 10 min, before being pelleted for 3 min at 8,000 × G and re-suspended in fresh YG broth for a 15 min chase period at 19 °C. Spores were imaged under a Zeiss Axiovert 200 M microscope with a Q-Imaging MicroPublisher 3.3 RTV camera. This experiment was repeated three times, with 20 spores observed in each occurrence.

2.6. Soluble protein extraction from *Z. tritici*

The following steps were carried out on ice and at 4 °C in the centrifuge. Samples from *Z. tritici* liquid cultures were centrifuged in 2 ml micro-centrifuge tubes at 20,000g for 10 min and the supernatant removed. Cells were washed with 1 ml ice-cold MilliQ water and the centrifugation repeated. Cell pellets were re-suspended in 500 µl ice-cold breaking buffer (100 mM Tris [pH 7.5], 1 mM DTT, 10 % v/v Glycerol, 1 mM EDTA, 0.01 % SDS) containing Pierce Protease Inhibitor Tablets (ThermoFisher Scientific), and pooled into a screw cap tube. Samples were centrifuged for 10 min at 20,000g, the supernatant removed and the pellets stored at -20 °C.

Cells were thawed on ice and re-suspended in a volume of breaking buffer equal to the cell pellet. Glass beads were added to just below the meniscus layer and the cells lysed using a FastPrep-24™ Classic Instrument (MP Biomedicals), with four runs of 20 sec at 6.5 m/s, interspaced with 1 min intervals of cooling samples on ice. Following cell lysis, the cell debris and glass beads were pelleted by centrifugation at 13,000g for 10 min. The supernatant was then transferred to a 1.5 ml micro-centrifuge tube and the centrifugation repeated to clarify the protein extract. The total protein concentration was determined using the Pierce™ Coomassie (Bradford) Protein Assay Kit (ThermoFisher Scientific) following the manufacturer's instructions.

2.7. Western blotting

Western blots were carried out using 30 µg of each protein sample in 20 µl of breaking buffer, to which 5 µl of NuPAGE™ LDS Sample Buffer (Invitrogen) and 1 µl 0.5 M dithiothreitol (DTT) was added. Samples were denatured at 70 °C for 10 min before being loaded onto a 10 % NuPAGE™ Bis-Tris Gel (Invitrogen) and separated by electrophoresis at 200 V in NuPAGE™ MOPS buffer (Invitrogen). Proteins were transferred to a PVDF membrane in NuPAGE™ Transfer Buffer (Invitrogen) following manufacturers instructions. The membrane was then washed in TBS (10 mM Tris-HCl pH8, 137 mM NaCl) before protein transfer and equal protein loading was assessed using Ponceau S stain (0.1 % Ponceau S, 5 % Acetic acid). Ponceau S was washed from the membrane using 100 mM NaOH and rinsed thoroughly with TBS.

The membrane was blocked by incubation in 25 ml TBS-T (TBS amended with 0.1 % Tween-20) containing 5 % milk powder (TBS-T + M) overnight at 4 °C. The membrane was then stained in 25 ml TBS-T + M containing 200 ng/ml GFP Polyclonal Antibody (Invitrogen) overnight at 4 °C. The membrane was washed four times with TBS-T for 5 min and stained with 25 ml TBS-T + M containing 50 ng/ml Goat anti-Rabbit IgG (H + L) Cross-Adsorbed Secondary Antibody, HRP (Invitrogen) for 1 h at room temperature. After washing with TBS-T, SuperSignal™ West Pico Chemiluminescent Substrate (Thermo Scientific) was applied to the membrane according to manufacturer's guidelines.

2.8. Growth assays under *in vitro* starvation

To assess the hyphal growth of *Z. tritici* under starvation, blastospores were harvested from YPD agar plates, filtered through a 100 µm cell strainer and washed twice with SDW. To quantify hyphal germination efficiency under starvation, cell suspensions were diluted to 5x10⁴ spores/ml before 500 µl was spread onto 2 % water agar plates and allowed to dry. The presence of hyphae emanating from 100 spores was assessed microscopically after incubation at 19 °C for 48 h. The experiment was repeated three times. The hyphal growth rate of *Z. tritici* strains was assessed on AMM, which was adjusted to create a growth medium lacking a carbon source (AMM C-) without glucose or a nitrogen source (AMM N-) without ammonium heptamolybdate and ammonium nitrate. Spore suspensions were diluted to a concentration of 5x10⁶ and 5 µl droplets were plated onto AMM, AMM C- and AMM N- agar plates. Radial growth was assessed after 14 d at 19 °C and the experiment repeated 3 times.

2.9. Virulence assay

Wheat seedlings (cultivar Riband) were grown in Levington M2 compost with a 3:1 addition of vermiculite, at 18 °C and 85 % relative humidity under a 12:12 h light:dark cycle in a Fitotron SG120 growth chamber (Weiss Technik, UK). *Z. tritici* blastospores were harvested from YPD agar plates and suspended in SDW containing 0.01 % (v/v) Tween 20. Blastospores were filtered through a 100 µm cell strainer, before being diluted to a concentration of 5x10⁶ and inoculated by the previously described method (Motteram et al., 2009). Disease symptoms were assessed at 21 days post infection (dpi), at which point the infected section of leaves was harvested and kept in a falcon tube containing 1 ml SDW overnight. Leaves were imaged using an Epson Perfection V850 Pro scanner. For quantitative assessment of virulence, pycnidia counts and infected leaf surface area were calculated using ImageJ to quantify pycnidia density. At least 3 leaves were infected in each of three technical replicates of the experiment for each strain analysed. Symptom development by mutant strains was compared to its isogenic background strain and mock leaves inoculated with 0.01 % Tween 20.

3. Results

3.1. Identification of candidate autophagy genes in *Z. tritici*

Analysis of the *Z. tritici* genome identified homologs of 27 ATG genes from *S. cerevisiae* and *M. oryzae* (Fig. 1; Table S2). These results were largely in agreement with a recent study of autophagy genes in 331 fungal species (Q. Wang et al., 2019), except for the identification of *ZtATG10*, *ZtATG14* and *ZtATG37* here (Fig. 1). Homologs of the pexophagy protein ATG37 and the E2-like enzyme ATG10 involved in the ATG12-conjugation complex were absent from the original JGI annotation of the *Z. tritici* genome. However, homologs of these proteins were identified here in the recent genome annotation from Rothamsted Research (King et al., 2017). Additionally, *ZtATG14* was identified using the sequence of a divergent homolog of *ScATG14* recently identified in *M. oryzae* and conserved in filamentous ascomycetes (Liu et al., 2017).

The *ZtATG* genes identified encode homologs of all the core machinery involved in autophagy in *S. cerevisiae*, apart from the phosphoprotein ATG31, which forms part of the Atg17-Atg31-Atg29 complex that acts as a scaffold for recruitment of ATG proteins to the PAS (Fig. 1a; Kabeya et al., 2009). Furthermore, the ATG29 homologs identified in *Z. tritici* (*ZtATG29*; ZtritIPO323_04g04445; 464 amino acids) and *M. oryzae* (*MoATG29*; MGG_02790; 443 amino acids) are significantly larger than *ScATG29* (YPL166W; 213 amino acids) and show only low homology at the N- and C-terminus (Table S2), indicating considerable divergence in the Atg17-Atg31-Atg29 complex in filamentous ascomycetes in comparison to yeast.

Genes encoding homologs of six proteins required for selective forms of autophagy in yeast were identified in the *Z. tritici* genome (Fig. 1b; Table S2). The predicted *Z. tritici* protein identified with sequence similarity to *ScATG20/Snx42*, ZtritIPO323_04g0743, displayed higher identity with *ScSnx41* and was therefore designated *ZtSnx41*. This gene likely fulfils the roles of both yeast sorting nexins *Snx41* and *Snx42/ScATG20* in pexophagy and endosomal retrieval trafficking, as was found for the *M. oryzae* protein *MoSnx41* (Deng et al., 2013). However, no evidence was found for the conservation of the yeast Cvt pathway in *Z. tritici*, in the absence of homologs of the Cvt-specific genes *ATG19*, *ATG23* and *ATG34* (Fig. 1b; Table S2), consistent with findings in other filamentous ascomycetes (Wang et al., 2019). Despite this, recent evidence for disrupted maturation of vacuolar aminopeptidase 1 (*Ape1*), a well characterised cargo protein of yeast Cvt pathway, in $\Delta atg1$ and $\Delta atg20$ of *A. oryzae* and *F. graminearum*, respectively, has suggested the presence of a distinct Cvt pathway in filamentous fungi (Lv et al., 2020; Yanagisawa et al., 2013). Searches for homologs of *ScATG18* and *ScATG21* identified the same *Z. tritici* gene, ZtritIPO323_04g13426, although the predicted protein showed higher sequence identity with *ScATG18*, and was hence designated *ZtATG18* (Table S2). This may explain the previous identification of *ScATG21* homologs in all fungal classes (Wang et al., 2019), although the role of these genes in the Cvt pathway of these species is yet to be determined.

Considering the essential role of their yeast homologs in both nonselective and selective forms of autophagy, the *Z. tritici* genes *ZtATG1* and *ZtATG8* were selected for further analysis (Fig. 1). tBLASTn searches confirmed the absence of any unannotated homologues of these

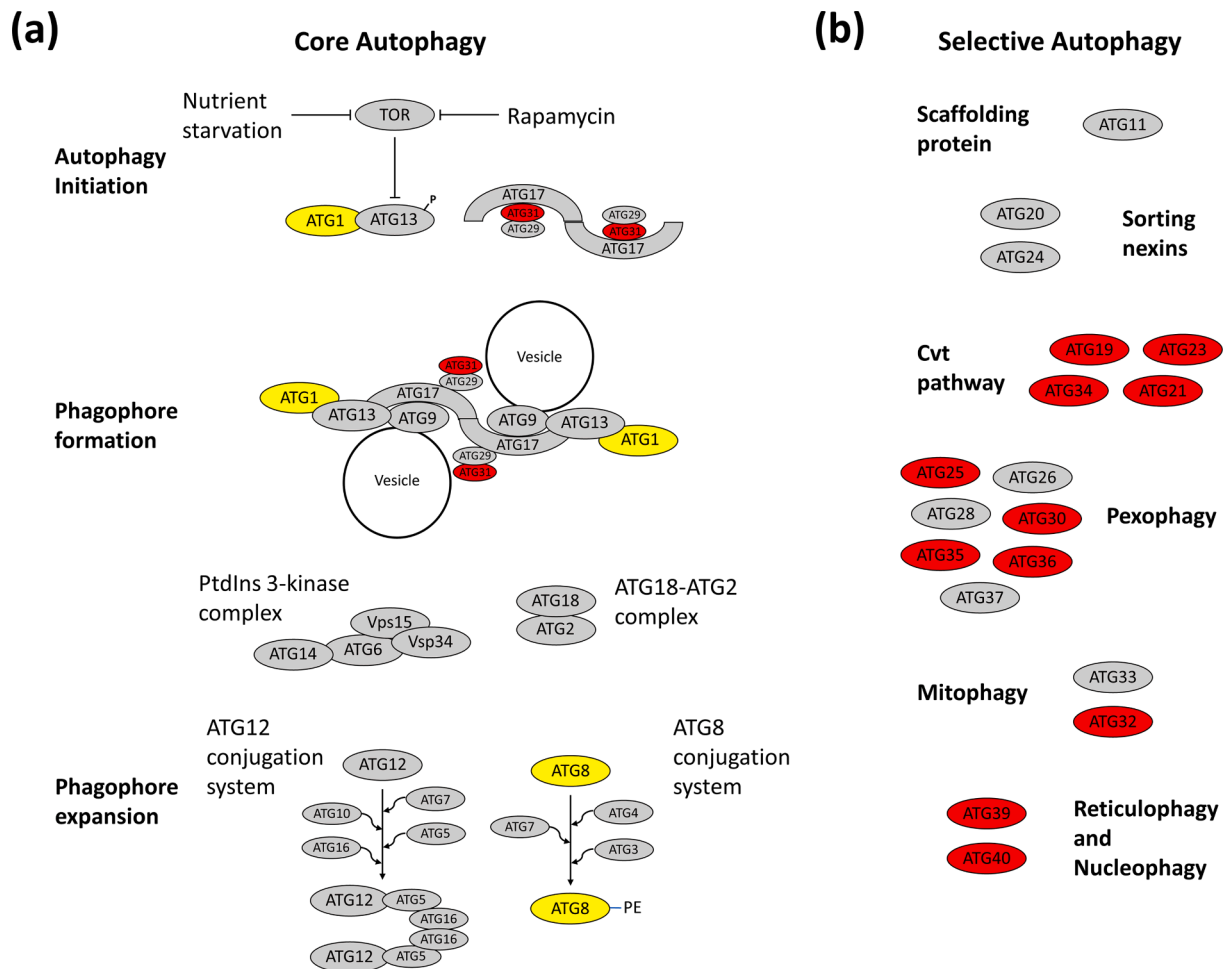


Fig. 1. Autophagy genes in *Z. tritici*. Schematic of the core (a) and selective (b) autophagy machinery from yeast species, coloured by those with (grey) and without (red) homologs in *Z. tritici*, and those investigated in this study (yellow).

genes in the *Z. tritici* genome. Gene models for ZtATG8 differ between the recent RRes and MPI annotations in the prediction of the first intron (Fig. S1a). Pairwise alignments with the MoATG8 and ScATG8 proteins and alignments of RNA sequencing reads from *Z. tritici* IPO323 in YPD cultures confirmed the correct intron boundaries from the Zt09_TU_chr_2_00900 model (Fig. S1), which was used for further analysis. Both ZtATG1 and ZtATG8 show high sequence identity with their homologs in *S. cerevisiae* and *M. oryzae* (Table S2; Fig. S1a; Figure S2), suggesting their conserved function in *Z. tritici* autophagy.

3.2. *Z. tritici* autophagy is active under nutrient-rich conditions and inhibited by deletion of ZtATG1

Targeted deletion of ZtATG1 and ZtATG8 was carried out to determine the function of autophagy in *Z. tritici* cellular differentiation and virulence. Wild type *Z. tritici* IPO323 was transformed with the plasmids pC-HYG-ATG1KO and pC-HYG-ATG8KO, resulting in replacement of ZtATG1 and ZtATG8 with the *HYG^R* selective marker through homologous recombination (Fig. 2A-B). Correct insertion of the selective marker and absence of the native coding sequences was confirmed by PCR (Fig. 2A-B), and three independent $\Delta ztatg1$ and $\Delta ztatg8$ strains were isolated.

The activity of autophagy can be monitored through the fluorophore-tagging of ATG8. This ubiquitin-like protein is associated with the autophagosome from its formation to its breakdown in the vacuole, enabling observation of autophagy from initiation to completion (Torggler et al., 2017). Therefore, to confirm the inhibition of autophagy in $\Delta ztatg1$, the vector pC_SUR_GFPATG8 was transformed into $\Delta ztatg1$ (Fig. 2C). This vector contains a cassette for expression of a ZtGFP:ZtATG8 N-terminal fusion protein, which is under the control of the endogenous ZtATG8 promoter and targeted to its native locus in the *Z. tritici* genome (Fig. 2C). The $\Delta ztatg8$ deletion strain was also transformed with pC_SUR_GFP:ATG8, replacing the *hygR* resistant marker with the ZtGFP:ZtATG8 fusion at its native locus (Fig. 2D). This was

done to visualise autophagy progression in wild type *Z. tritici*. Resulting strains also provided a complementation assay for any phenotype identified in $\Delta ztatg8$ and confirmed the wild type functionality of the ZtGFP:ZtATG8 fusion protein.

Localisation of ZtGFP:ZtATG8 was observed in wild type ZtGFP:ZtATG8 and $\Delta ztatg1$ ZtGFP:ZtATG8 cells after 5 days growth on YPD plates (Fig. 3). Cells were stained with FM4-64 to visualise the vacuolar membrane and assess autophagosome delivery to the lytic compartment. In wild type cells, ZtGFP:ZtATG8 fluorescence was observed at small puncta, indicating the formation of autophagosomes, as well as more dispersed regions of lower intensity fluorescence within the vacuolar membrane, indicating the delivery of ZtGFP:ZtATG8 into the vacuole through autophagy (Fig. 3). This suggests that *Z. tritici* is actively undergoing autophagy even during growth by blastosporeulation in nutrient-rich conditions. Conversely, ZtGFP:ZtATG8 was localised at bright puncta in $\Delta ztatg1$ cells, but was never observed to be dispersed within the vacuolar membrane (Fig. 3), indicating that ZtGFP:ZtATG8 is not being transported into the vacuole. This indicates that while ATG proteins are accumulating at the PAS in $\Delta ztatg1$ cells, any resulting autophagosomes are not being transported to the vacuole, suggesting that autophagy is blocked in these mutants.

To support the observation of inhibited vacuolar delivery of ZtGFP:ZtATG8 in $\Delta ztatg1$ from microscopic analysis, western blot assays were carried out to assess the degradation of ZtGFP:ZtATG8 (Fig. 4). Upon release of GFP:ATG8 proteins into the vacuole, proteolysis of the ATG8 moiety leads to the release of free-GFP, which is more stable under protease activity (Torggler et al., 2017). This enables assessment of autophagic flux by quantifying the relative abundance of the 41 kDa ZtGFP:ZtATG8 band and the 27 kDa free-GFP. ZtGFP:ZtATG8 and $\Delta ztatg1$ ZtGFP:ZtATG8 were grown for 5 d on YPD agar plates before being suspended in YPD broth at 5×10^6 spores/ml and incubated at 19 °C for 24 h. Total protein was extracted and analysed by western blotting with an anti-GFP antibody. In the wild type background, full length ZtGFP:ZtATG8 protein was detected alongside free-GFP (Fig. 4),

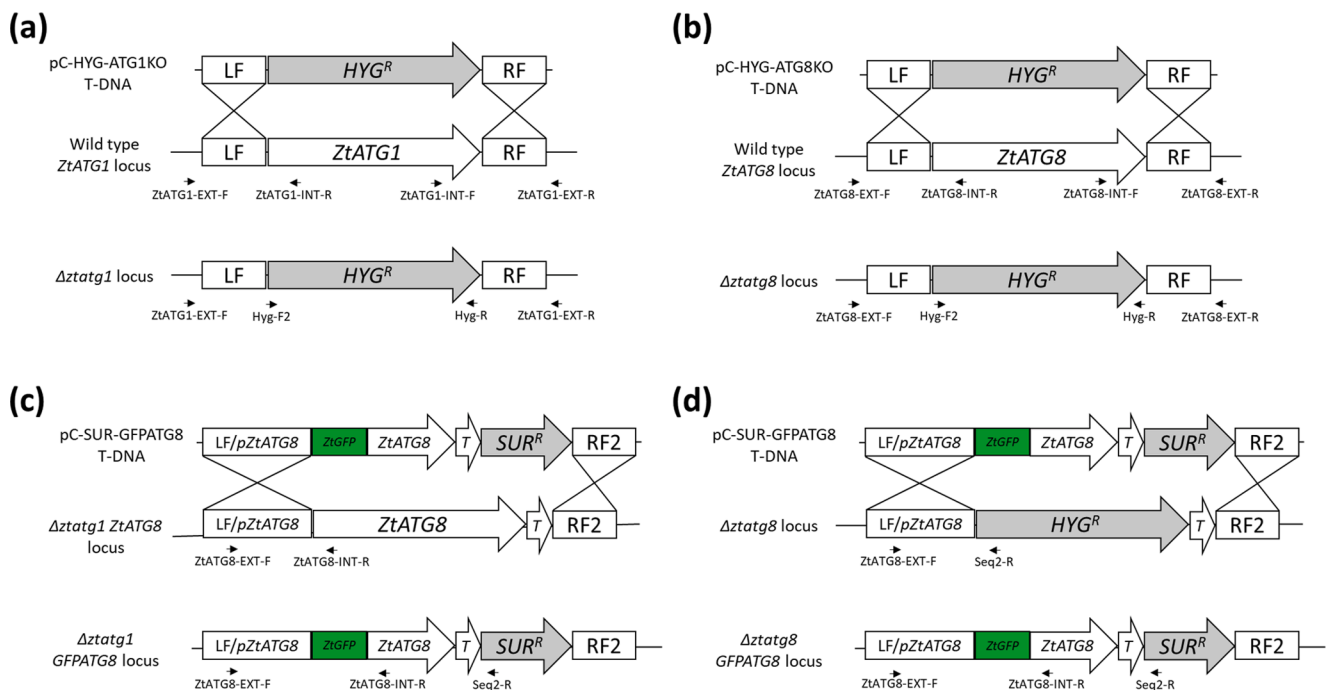


Fig. 2. Targeted deletion of *Z. tritici* autophagy genes ZtATG1 and ZtATG8 and expression of a ZtGFP:ZtATG8 fusion. Schematics displaying homologous recombination between flanking sequences (LF and RF) of T-DNA from the plasmids pC-HYG-ATG1KO (a), pC-HYG-ATG8KO (b) and pC-SUR-GFPATG8 (c and d) and the targeted loci in the *Z. tritici* genome, with resulting transgenic loci below. Depicted sequences include the ZtATG8 promoter (pZtATG8) and terminator (T), and the codon-optimised GFP (ZtGFP; Kilaru et al 2015). Primers (arrows) used for PCR screening of resulting transformants are shown below their respective target loci (sequences in Table S1).

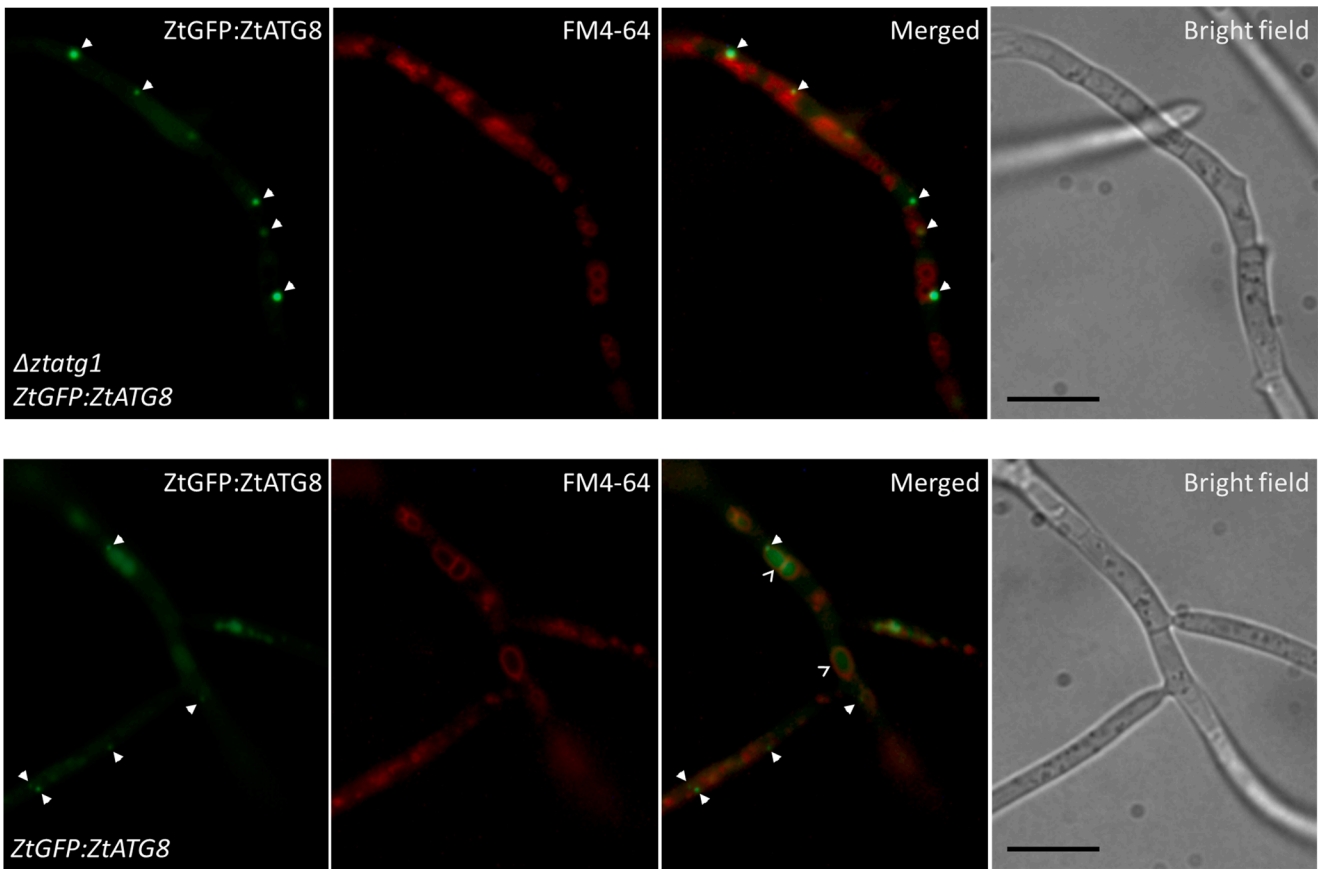


Fig. 3. Vacuolar localisation of ZtGFP:ZtATG8 is abolished in $\Delta zttatg1$ cells. Localisation of ZtGFP:ZtATG8 fluorescence within FM4-64 stained vacuoles of ZtGFP:ZtATG8 cells (open arrowheads), which is not observed in $\Delta zttatg1$ cells expressing ZtGFP:ZtATG8. ZtGFP:ZtATG8 puncta, seen in both wild type and $\Delta zttatg1$ cells, are indicated by closed arrowheads. Scale bars = 10 μ m.

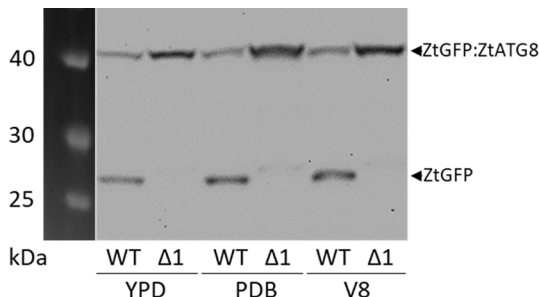


Fig. 4. Autophagic breakdown of ZtGFP:ZtATG8 is abolished in $\Delta zttatg1$ cells. ZtGFP:ZtATG8 breakdown releasing free-ZtGFP (27 kDa) protein in wild type (WT) and $\Delta zttatg1$ ($\Delta 1$) background cells grown for 24 h in yeast extract peptone dextrose broth (YPD), potato dextrose broth (PDB) and V8 juice broth (V8). This experiment was repeated three times.

indicating that autophagic delivery of ZtGFP:ZtATG8 is occurring during growth in nutrient-rich medium. This result was consistent in both potato dextrose broth and V8 juice (Campbell Foods, Puurs, Belgium) broth (Fig. 4), indicating that this finding is not limited to YPD. Furthermore, while full length ZtGFP:ZtATG8 was present, no free-GFP was observed in the $\Delta zttatg1$ background (Fig. 4), corroborating with microscopic evidence of inhibited autophagy in this mutant.

Consistent with the role of autophagy in the starvation response, GFP:ATG8 proteins have been shown to break down when filamentous fungi are transferred to nutrient-limited media (Liu et al., 2017; Lv et al., 2017). *Z. tritici* blastospores washed twice with sterile deionised water (SDW) and suspended in sterile water at 5×10^6 spores/ml. Total protein

was extracted from cells at 3 h intervals for 24 h. Autophagic ZtGFP:ZtATG8 cleavage did not increase in the wild type background over 24 h and remained absent in the $\Delta zttatg1$ background (Figure S3), suggesting that autophagic flux does not increase in *Z. tritici* upon exposure to starvation conditions.

3.3. Autophagy is not required for germination or growth under starvation in *Z. tritici*

As autophagy is important for cellular differentiation and growth under starvation in other fungal species, the involvement of ZtATG1 and ZtATG8 in the morphological switch to hyphal growth in response to nutrient deprivation was investigated. The rate of hyphal germination was unchanged in $\Delta zttatg1$ and $\Delta zttatg8$ compared to IPO323, with all strains displaying a mean germination efficiency over 90 % after 48 h on water agar (Fig. 5A). This suggests that autophagy is not essential for the hyphal transition in *Z. tritici*. To investigate growth rate during nutrient starvation, $\Delta zttatg1$ and $\Delta zttatg8$ strains were grown on minimal medium deficient in either a nitrogen or carbon source. The radial growth rate of the autophagy mutants was equivalent to the wild type over 14 days in all conditions analysed (Fig. 5B). However, $\Delta zttatg8$ strains showed slightly reduced hyphal density in radial colonies grown on carbon-depleted medium and displayed altered melanisation on nitrogen depleted medium (Fig. 5B). Both of these phenotypes were reversed in $\Delta zttatg8$ ZtGFP:ZtATG8 complementation strains (Fig. 5B). This provides evidence that autophagy plays no significant role in starvation induced hyphal growth in *Z. tritici*, while ZtATG8 deletion has a minor effect on growth morphology under these conditions.

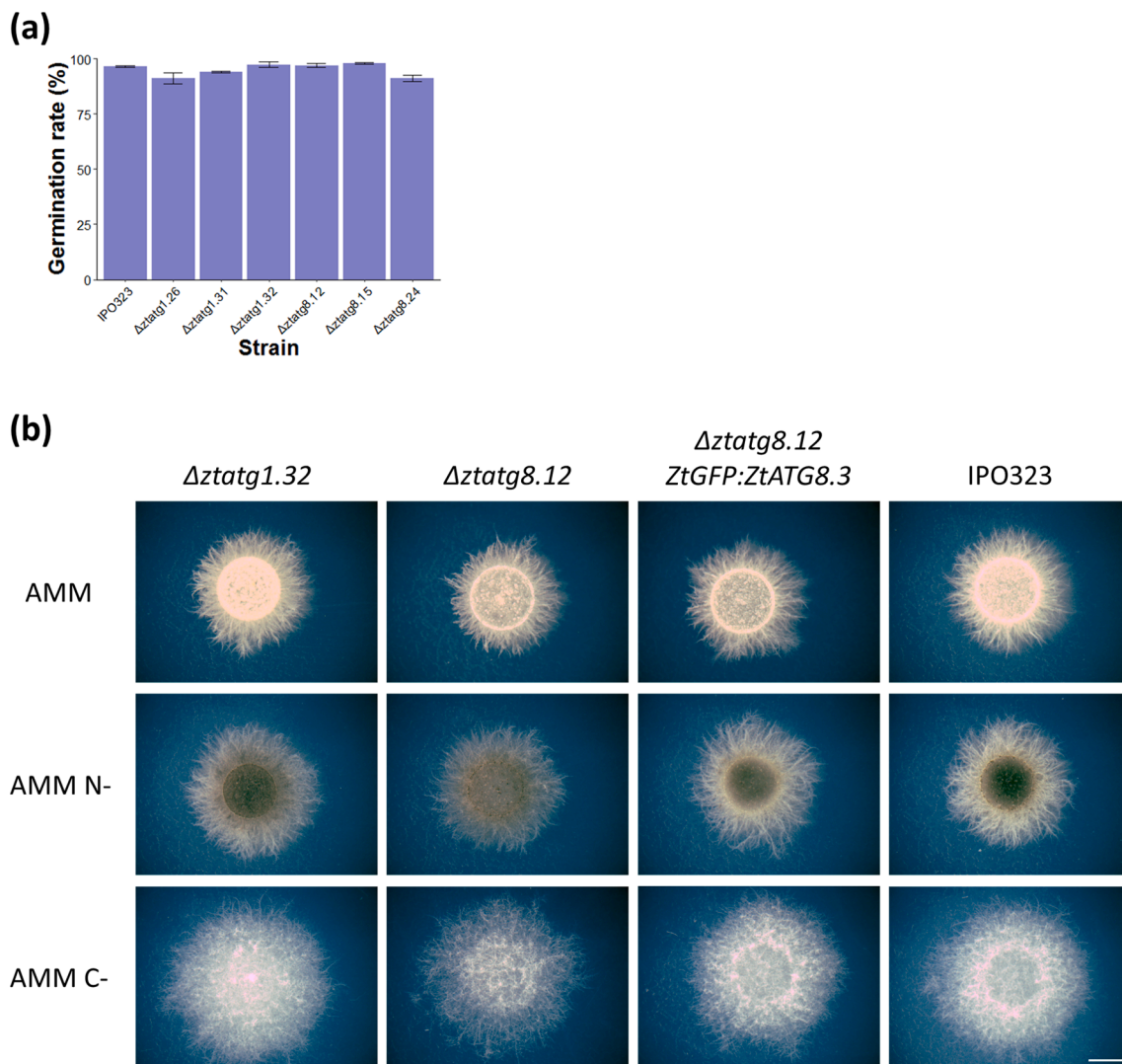


Fig. 5. Autophagy is not required for starvation induced hyphal growth. (a) Mean hyphal germination rate for each strain on water agar after 48 h (error bars = standard error). No significant difference between means identified by one-way ANOVA ($n = 4$). (b) Radial growth of autophagy mutants on *Aspergillus* minimal medium (AMM) and AMM deficient in nitrogen (AMM N-) and carbon (AMM C-) source. Plated in 5 μ l droplets of 5×10^6 spores/ml suspension and grown for 14 days at 19 °C. Scale bar = 2 mm.

3.4. Disruption of autophagy causes increased susceptibility to oxidative stress

Considering previous reports of the role of autophagy in the oxidative stress response in other filamentous fungi (Meng et al., 2020; Nitsche et al., 2013; Ying et al., 2016), the sensitivity of $\Delta zta1$ and $\Delta zta8$ to hydrogen peroxide was assessed. Growth of *Z. tritici* on YPD was inhibited under oxidative stress induced by hydrogen peroxide at concentrations above 4 mM (Fig. 6), which was consistent with previous studies (Yemelin et al., 2017; Francisco et al., 2019). While yeast-like growth of $\Delta zta1$ and $\Delta zta8$ was equivalent to the wild type on YPD, the inhibitory effect of hydrogen peroxide was enhanced in these mutants (Fig. 6). This phenotype was subtle but reproducible, and increased sensitivity to hydrogen peroxide was not observed in $\Delta zta8$ ZtGFP:ZtATG8 complementation strains. This suggests that autophagy is involved in maintaining cell viability and growth under oxidative stress in *Z. tritici*.

3.5. Autophagy is not required for *Z. tritici* pathogenicity, but ZtATG8 deletion reduces virulence.

Deletion of ZtATG1 and ZtATG8 did not inhibit the ability of *Z. tritici* to complete its asexual infection cycle on susceptible wheat leaves. $\Delta zta1$ and $\Delta zta8$ strains were able to cause necrosis and form pycnidia on infected leaf tissue 21 days after inoculation (Fig. 7A). This provides evidence that autophagy is not required for infection-related development of *Z. tritici*. However, leaves infected with $\Delta zta8$ strains displayed a significant reduction in pycnidia density compared to IPO323 and $\Delta zta8$ ZtGFP:ZtATG8 complementation strains at this stage, which was not identified in $\Delta zta1$ strains (Fig. 7B). Despite this, leaves infected with $\Delta zta8$ strains were covered with pycnidia-bearing necrotic lesions by 28 dpi (Fig. 7A). This is consistent with a delay in the onset of the necrotrophic phase in leaves infected with $\Delta zta8$ strains, which was observed during daily inspection of symptom development. These findings suggest that, while autophagy is not required for the pathogenicity of *Z. tritici*, ZtATG8 has an autophagy-independent role in supporting full virulence of this pathogen.

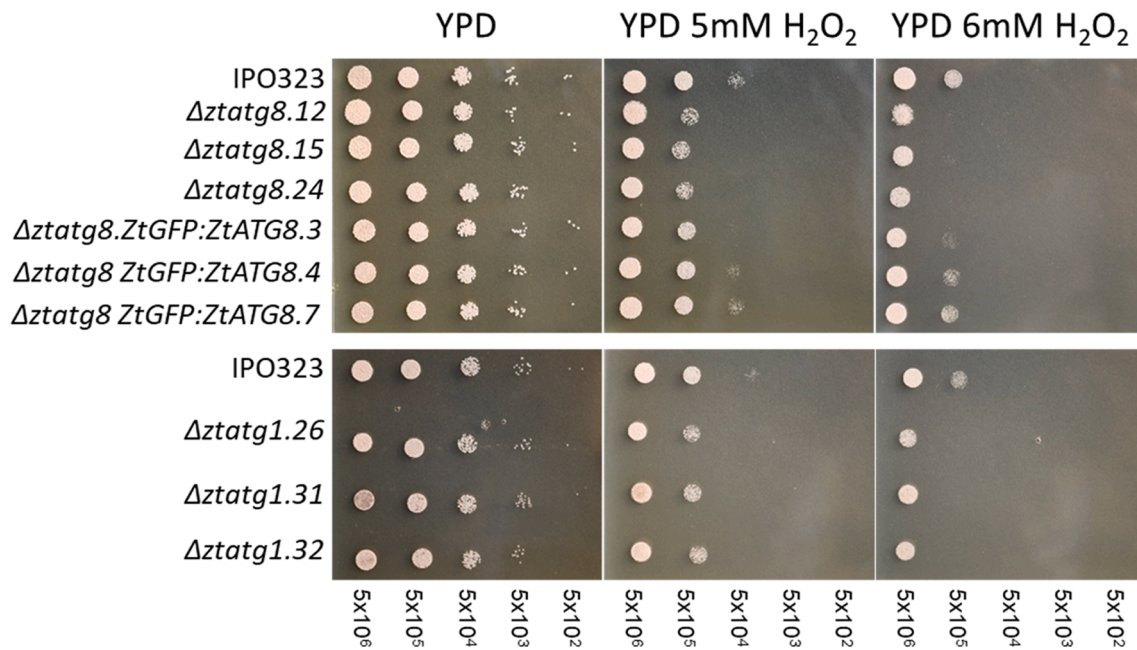


Fig. 6. *Δzttatg1* and *Δzttatg8* strains show increased sensitivity to oxidative stress. *Z. tritici* strains plated onto YPD containing hydrogen peroxide H_2O_2 at increasing concentrations. Spore suspensions prepared in 10-fold dilution series down from 5×10^6 spores/ml and plated in 5 μ l droplets. This experiment was repeated three times.

4. Discussion

To our knowledge, autophagy has been found to contribute to the virulence of all fungal plant pathogens in which it has been characterised to date (Asakura et al., 2009; Corral-Ramos et al., 2015; Josefsen et al., 2012; Kershaw & Talbot, 2009; Meng et al., 2020; Nadal & Gold, 2010; Ren et al., 2017; Shi et al., 2019; Sumita et al., 2017; Zhan et al., 2017). In the present study, the *Z. tritici* genome was found to encode a similar complement of autophagy genes as previously identified in the filamentous pathogens *M. oryzae* and *F. graminearum* (Kershaw & Talbot, 2009; Liu et al., 2017; Lv et al., 2017). Furthermore, deletion of *ZtATG1* was shown to block autophagy in *Z. tritici*, with mutants defective in the transport of autophagosome-bound ZtGFP:ZtATG8 to the vacuole for degradation. The ZtGFP:ZtATG8 puncta observed in *Δzttatg1* cells likely represent its accumulation at the PAS, which has also been seen to occur in *Δatg1* strains of *S. cerevisiae* (Cheong et al., 2008; Suzuki et al., 2001) and *F. graminearum* (Lv et al., 2017). However, *Δzttatg1* strains remained fully virulent towards wheat leaves, displaying equivalent symptoms and asexual development to the wild type. This suggests that autophagy is dispensable for *Z. tritici* virulence, in contrast to all other fungal plant pathogens studied to date.

Although there have been reports of the formation of appressorium-like swellings by *Z. tritici* hyphae (Duncan & Howard, 2000), host invasion is thought not to require the development of complex penetration structures, for which autophagy is required in other plant pathogens (Asakura et al., 2009; Liu et al., 2007; Ren et al., 2017). Despite this, the previously characterised role of autophagy in hyphal germination and growth under starvation conditions in filamentous fungi is relevant to *Z. tritici* infection, as early colonisation by this fungus is thought to require recycling of stored nutrients for epiphytic growth and initial colonisation of the apoplast (Rudd et al., 2015; Sánchez-Vallet et al., 2015). However, *Δzttatg1* strains showed no defect in the morphological switch to filamentous growth under starvation. Furthermore, autophagic breakdown of ZtGFP:ZtATG8 was not observed to increase during exposure to starvation conditions. This suggests that autophagy is not

required for this process, and that other mechanisms for mobilising internal energy stores can still drive filamentation.

Autophagic flux, monitored through GFP:ATG8 cleavage assays, has been shown to be repressed under nutrient rich conditions and activated under starvation in the yeasts *S. cerevisiae* and *Candida glabrata* (Meiling-Wesse et al., 2002; Shimamura et al., 2019), as well as the filamentous fungus *Aspergillus nidulans* (Pinar et al., 2013). Contrastingly, results in this study suggest that autophagic flux is active in *Z. tritici* during growth on rich media and is not influenced by starvation. Breakdown of GFP:ATG8 has also been observed under nutrient rich conditions in the filamentous fungi *M. oryzae* and *F. graminearum*, although in both cases this was enhanced under starvation (Liu et al., 2017; Lv et al., 2017). These results may suggest that autophagy is constitutively active in these species, perhaps for the distribution of nutrients required for growth, or that the nutrient replete conditions used in laboratory culture exert some stress on growing cells to induce autophagy.

Autophagy is proposed to be a precursor to autolytic cell death in aging mycelial compartments to facilitate the recycling of nutrients to the growing tip in *A. oryzae* (Shoji & Craven, 2011). Similarly, autophagy is required for developmentally-regulated programmed cell death in the conidia of *M. oryzae*, the contents of which are transported to the developing appressorium (Veneault-Fourrey et al., 2006). However, there is accumulating evidence that epiphytic compartments of *Z. tritici* play an important role in the infection cycle. Pycnidiospores have been demonstrated to undergo budding to produce blastospores on the leaf surface, which is proposed to provide a source of secondary inoculum without the completion of the invasive infection cycle (Francisco et al., 2019). Experiments using leaf surface-acting fungicides to kill epiphytic hyphae have also demonstrated their contribution to virulence up to 7 days after inoculation (Fones et al., 2017). Furthermore, avirulent *Z. tritici* strains can contribute to sexual reproduction despite their inability to colonise the leaf tissue (Kema et al., 2018), suggesting that their persistence on the leaf surface may enable them to undergo mating (Suffert et al., 2019). Unselective autophagy of bulk cytoplasm will lead to the degradation of organelles as well as lipid stores (Kiššová et al.,

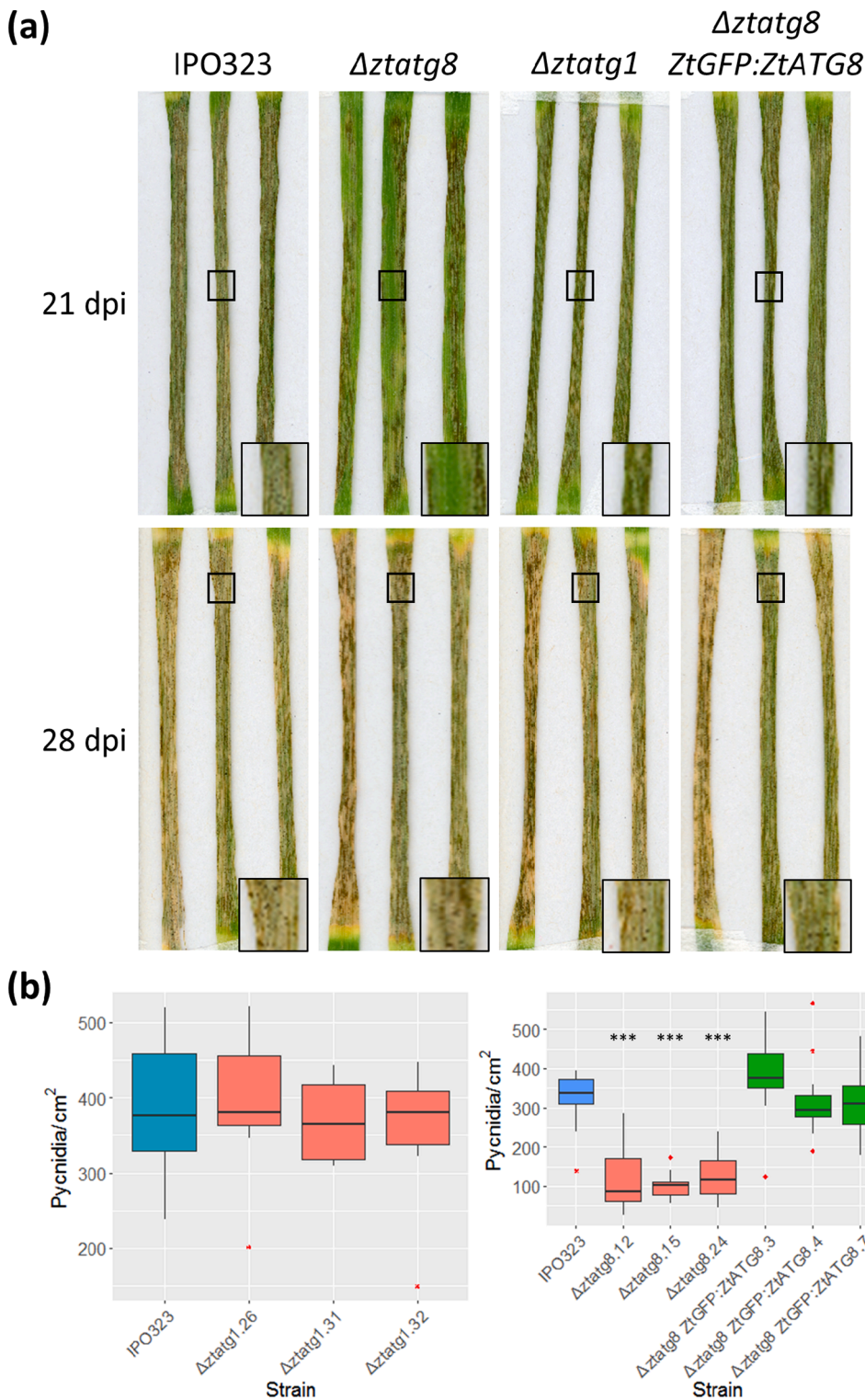


Fig. 7. $\Delta ztatg8$ is delayed in causing symptoms during infection of wheat leaves. (a) Wheat leaves infected with *Z. tritici* at 5×10^6 spores/ml after 21 and 28 days post infection (dpi). A magnified image of the region in the black box is included as an inset in the bottom right of each image. (b) Pycnidia density on infected leaves after 21 dpi. Significant differences between mean pycnidia density on leaves infected with IPO323 and others strains determined by one-way ANOVA and subsequent pairwise comparisons with a Tukey post hoc test, identifying significant reduction ($***p < 0.001$) in pycnidia density of $\Delta ztatg8$ infected leaves, which was reversed in $\Delta ztatg8$ ZtGFP:ZtATG8 strains.

2007; Shoji et al., 2010), which may be detrimental to epiphytic cell survival. Accordingly, there may be a disadvantage to intracellular degradation and autolytic death of epiphytic *Z. tritici* cells after germination and host penetration. This could explain the reduced reliance on autophagy for stored nutrient mobilisation in *Z. tritici* compared to other pathogens such as *M. oryzae*.

Z. tritici may therefore preferentially degrade LDs directly in the cytoplasm via the activity of TAG lipases. Crosstalk between lipolysis and autophagy has recently been elucidated in yeast and animal cells

(Maeda et al., 2015; Rambold et al., 2015; van Zutphen et al., 2014). Recent evidence suggests that mammalian cells favour mobilisation of fatty acids (FAs) from LDs through lipolysis over lipophagy under starvation conditions (Rambold et al., 2015). The authors proposed that lipophagy may lead to toxicity from increases in cytosolic FAs, while lipolysis allows direct flow of FAs from LDs to mitochondria, facilitated by the proximity of these organelles (Rambold et al., 2015). In contrast, *S. cerevisiae* cells were found to accumulate LDs in the vacuole during starvation, indicating that autophagy is important for energy

mobilisation under these conditions (van Zutphen et al., 2014). Furthermore, TAG lipase activity was found to be higher during stationary phase growth after deletion of the vacuolar lipase ATG15, indicating coordinated regulation of lipolysis and lipophagy in *S. cerevisiae* (Maeda et al., 2015). It is therefore possible that lipolysis is the primary method of LD breakdown in *Z. tritici*, or is at least able to complement the loss of lipophagy in this species.

Autophagy deficient mutants were also found to display increased sensitivity to hydrogen peroxide here, although this effect was not dramatic. Autophagy is known to be involved in the response to oxidative stress through the degradation of organelles and macromolecules damaged by reactive oxygen species (ROS; Filomeni et al., 2015). Furthermore, increased sensitivity to exogenous ROS is a common phenotype of autophagy deficient filamentous fungi (Meng et al., 2020; Nitsche et al., 2013; Ying et al., 2016). The influence of autophagy disruption on ROS sensitivity may be dampened by the activation of adaptive enzymatic responses to oxidative stress in autophagy mutants, exemplified by the increased superoxide dismutase activity in *S. cerevisiae* Δatg mutants (Zhang et al., 2007). The weak effect of autophagy disruption on ROS sensitivity observed here may reflect the capability of *Z. tritici* to withstand high levels of extracellular ROS during induction of host cell death (Keon et al 2007), which is thought to involve the activity of secreted chloroperoxidases and superoxide dismutase enzymes (Palma-Guerrero et al., 2016).

Although *Z. tritici* $\Delta ztatg1$ mutants were fully virulent, deletion of *ZtATG8* led to a delay in symptom development during infection. As autophagy was demonstrated to be inhibited by *ZtATG1* deletion without impacting virulence, this indicates the potential for autophagy-independent functions of *ZtATG8*. Distinct phenotypes of ATG8 knock-out strains have been observed in multiple fungal pathogen species, often involving more severe virulence defects in $\Delta atg8$ than $\Delta atg1$ strains (Duan et al., 2013; Nadal & Gold, 2010; Ying et al., 2016). However, the cellular mechanisms governing the disparity between the phenotypes of $\Delta atg1$ and $\Delta atg8$ mutants in these species remains to be characterised.

Multiple autophagy-independent functions of ATG8 have been identified in model yeast species. Deletion of ATG8 was found to impair vacuolar morphology under various stress conditions in *Pichia pastoris* (Tamura et al., 2010) and *Schizosaccharomyces pombe* (Liu et al., 2018; Mikawa et al., 2010), and the formation of vacuolar microdomains during the stationary phase in *S. cerevisiae* (Liu et al., 2018). These functions of ATG8 were independent of conjugation to PE (or lipidation), which is essential for its role in autophagosome formation (Fig. 1; Liu et al., 2018; Maeda et al., 2017). Crucially, these additional vacuolar functions of yeast ATG8 were dependant on environmental stress or growth phase (Liu et al., 2018; Tamura et al., 2010). *ZtATG8* may therefore influence vacuolar morphology in *Z. tritici* during infection under conditions not characterised *in vitro* in this study. Furthermore, ATG8 has been shown to bind to LDs in a lipidation-independent manner and maintain the quantity of LDs in stationary phase cells of *S. cerevisiae*, antagonising lipolysis by mediating LD clustering (Maeda et al., 2017). A similar role of *ZtATG8* in LD dynamics may influence invasive growth and therefore virulence of *Z. tritici* in a quantitative manner, which may reflect the minor changes in hyphal growth morphology identified here *in vitro*.

These findings provide potential mechanisms by which *ZtATG8* may carry out autophagy-independent functions that impact *Z. tritici* virulence. The localisation of *ZtATG8* to vacuolar and LD membranes should be assessed to investigate these possible functions. Additionally, the virulence phenotype of strains deficient in *ZtATG8* lipidation, through deletion of *ZtATG4* or *ZtATG7*, should be characterised to assess whether the delayed symptom development of $\Delta ztatg8$ strains is independent of defects in *ZtATG8* conjugation that inhibit autophagy.

5. Conclusions

In summary, the present study provides evidence that autophagy is not required for the germination and hyphal growth of *Z. tritici* under nutrient deprivation during early invasion of wheat, and is therefore dispensable for pathogenicity. This is contrary to the crucial function of autophagy in infection-related development identified in many other pathogenic fungi. Further study is required to understand how *Z. tritici* mobilises stored fatty acids from LDs to support growth under starvation, focusing on elucidating the role of cytosolic lipolysis and its potential crosstalk with autophagy in this process. Finally, deletion of *ZtATG8* was found to have a quantitative impact on *Z. tritici* virulence, warranting further investigation into the potential autophagy-independent functions of this gene.

CRedit authorship contribution statement

Harry T. Child: Methodology, Formal analysis, Investigation, Writing – original draft, Visualization, Project administration, Writing – review & editing. **Michael J. Deeks:** Writing – review & editing, Supervision. **Ken Haynes:** Conceptualization, Methodology, Funding acquisition, Supervision. **Jason J. Rudd:** Conceptualization, Methodology, Funding acquisition, Supervision. **Steven Bates:** Conceptualization, Methodology, Funding acquisition, Supervision, Project administration.

Declaration of Competing Interest

The authors declare that they have no known competing financial interests or personal relationships that could have appeared to influence the work reported in this paper.

Acknowledgements

This work was supported by the BBSRC-funded South West Biosciences Doctoral Training Partnership (BB/M009122/1) and Designing Future Wheat Institute Strategic Programme (BB/P016855/1) awarded to Rothamsted Research. We thank Professor Gero Steinberg and Dr Sreedhar Kilharu for providing the codon optimised ZtGFP plasmid.

Appendix A. Supplementary material

Supplementary data to this article can be found online at <https://doi.org/10.1016/j.fgb.2022.103748>.

References

- Asakura, M., Ninomiya, S., Sugimoto, M., Oku, M., Yamashita, S.-I., Okuno, T., Sakai, Y., Takano, Y., 2009. Atg26-Mediated Pexophagy Is Required for Host Invasion by the Plant Pathogenic Fungus *Colletotrichum orbiculare*. *Plant Cell* 21 (4), 1291–1304.
- Cheong, H., Nair, U., Geng, J., Klionsky, D.J., Subramani, S., 2008. The Atg1 Kinase Complex Is Involved in the Regulation of Protein Recruitment to Initiate Sequestering Vesicle Formation for Nonspecific Autophagy in *Saccharomyces cerevisiae*. *Mol. Biol. Cell* 19 (2), 668–681.
- Child, H.T., Helmstetter, N., 2009. *Agrobacterium*-mediated transformation of *Zygomycetia tritici*. *protocols.io*. <https://dx.doi.org/10.17504/protocols.io.b5ukq6uw>.
- Corral-Ramos, C., Roca, M.G., Pietro, A.D., Roncero, M.I.G., Ruiz-Roldán, C., 2015. Autophagy contributes to regulation of nuclear dynamics during vegetative growth and hyphal fusion in *Fusarium oxysporum*. *Autophagy* 11, 131–144. <https://doi.org/10.4161/15548627.2014.994413>.
- Deng, Y., Qu, Z., Naqvi, N.I., Chaturvedi, V., 2013. The role of Snx41-based pexophagy in *Magnaporthe* development. *PLoS ONE* 8 (11), e79128.
- Di Tommaso, P., Moretti, S., Xenarios, I., Orobitz, M., Montanyola, A., Chang, J.M., Taly, J.F., Notredame, C., 2011. T-Coffee: a web server for the multiple sequence alignment of protein and RNA sequences using structural information and homology extension. *Nucleic Acids Res* 39, W13–7.
- Duan, Z., Chen, Y., Huang, W., Shang, Y., Chen, P., Wang, C., 2013. Linkage of autophagy to fungal development, lipid storage and virulence in *Metarhizium robertsii*. *Autophagy* 9 (4), 538–549.
- Duncan, K.E., Howard, R.J., 2000. Cytological analysis of wheat infection by the leaf blotch pathogen *Mycosphaerella graminicola*. *Mycol. Res.* 104, 1074–1082. <https://doi.org/10.1017/S0953756299002294>.

- Feng, Y., He, D., Yao, Z., Klionsky, D.J., 2014. The machinery of macroautophagy. *Cell Res.* 24, 24–41. <https://doi.org/10.1038/cr.2013.168>.
- Filomeni, G., Zio, D.D., Cecconi, F., 2015. Oxidative stress and autophagy: the clash between damage and metabolic needs. *Cell Death Differ.* 22, 377–388. <https://doi.org/10.1038/cdd.2014.150>.
- Fones, H., Gurr, S., 2015. The impact of Septoria tritici Blotch disease on wheat: An EU perspective. *Fungal Genet. Biol.* 79, 3–7. <https://doi.org/10.1016/j.fgb.2015.04.004>.
- Fones, H.N., Eyles, C.J., Kay, W., Cowper, J., Gurr, S.J., 2017. A role for random, humidity-dependent epiphytic growth prior to invasion of wheat by *Zymoseptoria tritici*. *Fungal Genet. Biol.* 106, 51–60. <https://doi.org/10.1016/j.fgb.2017.07.002>.
- Francisco, C.S., Ma, X., Zwysig, M.M., McDonald, B.A., Palma-Guerrero, J., 2019. Morphological changes in response to environmental stresses in the fungal plant pathogen *Zymoseptoria tritici*. *Sci. Rep.* 9, 9642. <https://doi.org/10.1038/s41598-019-45994-3>.
- Ichimura, Y., Kirisako, T., Takao, T., Satomi, Y., Shimonishi, Y., Ishihara, N., Mizushima, N., Tanida, I., Kominami, E., Ohsumi, M., Noda, T., Ohsumi, Y., 2000. A ubiquitin-like system mediates protein lipidation. *Nature* 408 (6811), 488–492.
- Josefsen, L., Droce, A., Sondergaard, T.E., Sørensen, J.L., Bormann, J., Schäfer, W., Giese, H., Olsson, S., 2012. Autophagy provides nutrients for nonassimilating fungal structures and is necessary for plant colonization but not for infection in the necrotrophic plant pathogen *Fusarium graminearum*. *Autophagy* 8 (3), 326–337.
- Kabeya, Y., Noda, N.N., Fujioka, Y., Suzuki, K., Inagaki, F., Ohsumi, Y., 2009. Characterization of the Atg17-Atg29-Atg31 complex specifically required for starvation-induced autophagy in *Saccharomyces cerevisiae*. *Biochem. Biophys. Res. Commun.* 389, 612–615. <https://doi.org/10.1016/j.bbrc.2009.09.034>.
- Kema, G.H.J., Mirzadi Gohari, A., Aouini, L., Gibriel, H.A.Y., Ware, S.B., van den Bosch, F., Manning-Smith, R., Alonso-Chavez, V., Helps, J., Ben M'Barek, S., Mehrabi, R., Diaz-Trujillo, C., Zamani, E., Schouten, H.J., van der Lee, Waalwijk, C., de Waard, de Wit, P., Verstappen, E.C.P., Thomma, B., Meijer, H.J.G., Seidl, M.F., 2018. Stress and sexual reproduction affect the dynamics of the wheat pathogen effector AvrStb6 and strobilurin resistance. *Nat. Genet.* 50, 375–380.
- Kema, G.H.J., Yu, D.Z., Rijkenberg, F.H.J., Shaw, M.W., Baayen, R.P., 1996. Histology of the pathogenesis of *Mycosphaerella graminicola* in wheat. *Phytopathology* 86, 777–786. <https://doi.org/10.1094/Phyto-86-777>.
- Keon, J., Antoniow, J., Carzaniga, R., Deller, S., Ward, J.L., Baker, J.M., Beale, M.H., Hammond-Kosack, K., Rudd, J.J., 2007. Transcriptional adaptation of *Mycosphaerella graminicola* to programmed cell death (PCD) of its susceptible wheat host. *Mol. Plant Microbe Interact.* 20 (2), 178–193.
- Kershaw, M.J., Talbot, N.J., 2009. Genome-wide functional analysis reveals that infection-associated fungal autophagy is necessary for rice blast disease. *PNAS* 106, 15967–15972. <https://doi.org/10.1073/pnas.0901477106>.
- Khan, I.A., Lu, J.P., Liu, X.H., Rehman, A., Lin, F.C., 2012. Multifunction of autophagy-related genes in filamentous fungi. *Microbiol. Res.* 167, 339–345. <https://doi.org/10.1016/j.micres.2012.01.004>.
- Kilaru, S., Schuster, M., Studholme, D., Soanes, D., Lin, C., Talbot, N.J., Steinberg, G., 2015. A codon-optimized green fluorescent protein for live cell imaging in *Zymoseptoria tritici*. *Fungal Genet. Biol.* 79, 125–131.
- King, R., Urban, M., Lauder, R.P., Hawkins, N., Evans, M., Plummer, A., Halsey, K., Lovegrove, A., Hammond-Kosack, K., Rudd, J.J., Guo, H.-S., 2017. A conserved fungal glycosyltransferase facilitates pathogenesis of plants by enabling hyphal growth on solid surfaces. *PLoS Pathog.* 13 (10), e1006672.
- Kiššová, I.B., Salin, B., Schaeffer, J., Bhatia, S., Manon, S., Camougrand, N., et al., 2007. Selective and Non-Selective Autophagic Degradation of Mitochondria in Yeast ND ES RIB. *Autophagy* 4, 329–336. <https://doi.org/10.4161/auto.4034>.
- Klionsky, D.J., Baehrecke, E.H., Brumell, J.H., Chu, C.T., Codogno, P., Cuervo, A.M., Debnath, J., Deretic, V., Elazar, Z., Eskelinen, E.-L., Finkbeiner, S., Fucyo-Margareto, J., Gewirtz, D.A., Jäättelä, M., Kroemer, G., Levine, B., Melia, T.J., Mizushima, N., Rubinsztein, D.C., Simonsen, A., Thorburn, A., Thumm, M., Tooze, S. A., 2011. A comprehensive glossary of autophagy-related molecules and processes (2nd edition). *Autophagy* 7 (11), 1273–1294.
- Liu, X.-M., Yamasaki, A., Du, X.-M., Coffman, V.C., Ohsumi, Y., Nakatogawa, H., Wu, J.-Q., Noda, N.N., Du, L.-L., 2018. Lipidation-independent vacuolar functions of Atg8 rely on its noncanonical interaction with a vacuole membrane protein. *eLife* 7, e41237. <https://doi.org/10.7554/eLife.41237>.
- Liu, X.-H., Zhao, Y.-H., Zhu, X.-M., Zeng, X.-Q., Huang, L.-Y., Dong, B.O., Su, Z.-Z., Wang, Y., Lu, J.-P., Lin, F.-C., 2017. Autophagy-related protein MoAtg14 is involved in differentiation, development and pathogenicity in the rice blast fungus *Magnaporthe oryzae*. *Sci. Rep.* 7 (1) <https://doi.org/10.1038/srep40018>.
- Liu, X.H., Lu, J.P., Zhang, L., Dong, B., Min, H., Lin, F.C., 2007. Involvement of a *Magnaporthe grisea* serine/threonine kinase gene, MgATG1, in Appressorium turgor and pathogenesis. *Eukaryot. Cell* 6, 997–1005. <https://doi.org/10.1128/EC.00011-07>.
- Lv, W., Wang, C., Yang, N., Que, Y., Talbot, N.J., Wang, Z., 2017. Genome-wide functional analysis reveals that autophagy is necessary for growth, sporulation, deoxynivalenol production and virulence in *Fusarium graminearum*. *Sci. Rep.* 7, 11062. <https://doi.org/10.1038/s41598-017-11640-z>.
- Lv, W., Xu, Z., Talbot, N.J., Wang, Z., 2020. The sorting nexin FgAtg20 is involved in the Cvt pathway, non-selective macroautophagy, pexophagy and pathogenesis in *Fusarium graminearum*. *Cell. Microbiol.* 22, e13208.
- Lynch-Day, M.A., Klionsky, D.J., 2010. The Cvt pathway as a model for selective autophagy. *FEBS Lett.* 584, 1359–1366. <https://doi.org/10.1016/j.febslet.2010.02.013>.
- Maeda, Y., Oku, M., Sakai, Y., 2017. Autophagy-independent function of Atg8 in lipid droplet dynamics in yeast. *J. Biochem.* 161, 339–348. <https://doi.org/10.1093/jb/mvw078>.
- Maeda, Y., Oku, M., Sakai, Y., Maeda, Y., Oku, M., Sakai, Y., 2015. A defect of the vacuolar putative lipase Atg15 accelerates degradation of lipid droplets through lipolysis A defect of the vacuolar putative lipase Atg15 accelerates degradation of lipid droplets through lipolysis. *Autophagy* 11, 1247–1258. <https://doi.org/10.1080/15548627.2015.1056969>.
- Meiling-Wesse, K., Barth, H., Thumm, M., 2002. Cez1p/Aut11p/Cvt16p is essential for autophagy and the cvt pathway. *FEBS Lett.* 526, 71–76. [https://doi.org/10.1016/S0014-5793\(02\)03119-8](https://doi.org/10.1016/S0014-5793(02)03119-8).
- Meng, S., Xiong, M., Jagernath, J.S., Wang, C., Qiu, J., Shi, H., Kou, Y., 2020. UvAtg8-Mediated Autophagy Regulates Fungal Growth, Stress Responses, Conidiation, and Pathogenesis in *Ustilago indica*. *Rice* 13 (1). <https://doi.org/10.1186/s12284-020-00418-z>.
- Mikawa, T., Kanoh, J., Ishikawa, F., 2010. Fission yeast Vps1 and Atg8 contribute to oxidative stress resistance. *Genes Cells* 15, 229–242. <https://doi.org/10.1111/j.1365-2443.2009.01376.x>.
- Minina, E.A., Bozhkov, P.V., Hofius, D., 2014. Autophagy as initiator or executioner of cell death. *Trends Plant Sci.* 19, 692–697. <https://doi.org/10.1016/j.tplants.2014.07.007>.
- Mizushima, N., 2010. The role of the Atg1/ULK1 complex in autophagy regulation. *Curr. Opin. Cell Biol.* 22 (2), 132–139.
- Mizushima, N., Komatsu, M., 2011. Autophagy: Renovation of cells and tissues. *Cell* 147, 728–741. <https://doi.org/10.1016/j.cell.2011.10.026>.
- Mizushima, N., Levine, B., 2010. Autophagy in mammalian development and differentiation. *Nat. Cell Biol.* 12, 823–830. <https://doi.org/10.1038/ncb0910-823>.
- Motteram, J., Küfner, I., Deller, S., Brunner, F., Hammond-Kosack, K.E., Nürnberger, T., Rudd, J.J., 2009. Molecular characterization and functional analysis of MgNLP, the sole NPP1 domain-containing protein, from the fungal wheat leaf pathogen *Mycosphaerella graminicola*. *Mol. Plant Microbe Interact.* 22 (7), 790–799.
- Nadal, M., Gold, S.E., 2010. The autophagy genes atg8 and atg1 affect morphogenesis and pathogenicity in *Ustilago maydis*. *Mol. Plant Pathol* 11, 463–478. <https://doi.org/10.1111/j.1364-3703.2010.00620.x>.
- Nakatogawa, H., Ichimura, Y., Ohsumi, Y., 2007. Atg8, a Ubiquitin-like Protein Required for Autophagosome Formation, Mediates Membrane Tethering and Hemifusion. *Cell* 130, 165–178. <https://doi.org/10.1016/j.cell.2007.05.021>.
- Nakatogawa, H., Ohbayashi, S., Sakoh-Nakatogawa, M., Kakuta, S., Suzuki, S.W., Kirisako, H., Kondo-Kakuta, C., Noda, N.N., Yamamoto, H., Ohsumi, Y., 2012. The Autophagy-related Protein Kinase Atg1 Interacts with the Ubiquitin-like Protein Atg8 via the Atg8 Family Interacting Motif to Facilitate Autophagosome Formation. *J. Biol. Chem.* 287 (34), 28503–28507.
- Nguyen, L.N., Bormann, J., Le, G.T.T., Stärkel, C., Olsson, S., Nosanchuk, J.D., Giese, H., Schäfer, W., 2011. Autophagy-related lipase FgATG15 of *Fusarium graminearum* is important for lipid turnover and plant infection. *Fungal Genet. Biol.* 48 (3), 217–224.
- Nitsche, B.M., Burggraaf-Van Welzen, A.M., Lamers, G., Meyer, V., Ram, A.F.J., 2013. Autophagy promotes survival in aging submerged cultures of the filamentous fungus *Aspergillus niger*. *Appl. Microbiol. Biotechnol.* 97, 8205–8218. <https://doi.org/10.1007/s00253-013-4971-1>.
- Orvedahl, A., Levine, B., 2009. Eating the enemy within: Autophagy in infectious diseases. *Cell Death Differ.* 16, 57–69. <https://doi.org/10.1038/cdd.2008.130>.
- Palma-Guerrero, J., Torriani, S.F.F., Zala, M., Carter, D., Courbot, M., Rudd, J.J., McDonald, B.A., Croll, D., 2016. Comparative transcriptomic analyses of *Zymoseptoria tritici* strains show complex lifestyle transitions and intraspecific variability in transcription profiles. *Mol. Plant Pathol* 17 (6), 845–859.
- Parzych, K.R., Ariosa, A., Mari, M., Klionsky, D.J., Glick, B.S., 2018. A newly characterized vacuolar serine carboxypeptidase, Atg42/Ybr139w, is required for normal vacuole function and the terminal steps of autophagy in the yeast *Saccharomyces cerevisiae*. *Mol. Biol. Cell* 29 (9), 1089–1099.
- Pinan-Lucarré, B., Balguería, A., Clavé, C., 2005. Accelerated cell death in *Podospora* autophagy mutants. *Eukaryot. Cell* 4, 1765–1774. <https://doi.org/10.1128/EC.4.11.1765>.
- Pinar, M., Pantazopoulou, A., Peñalva, M.A., 2013. Live-cell imaging of *Aspergillus nidulans* autophagy. *Autophagy* 9 (7), 1024–1043. <https://doi.org/10.4161/auto.24483>.
- Pollack, J.K., Harris, S.D., Marten, M.R., 2009. Autophagy in filamentous fungi. *Fungal Genet. Biol.* 46, 1–8. <https://doi.org/10.1016/j.fgb.2008.10.010>.
- Rambold, A.S., Cohen, S., Lippincott-schwartz, J., Rambold, A.S., Cohen, S., Lippincott-schwartz, J., 2015. Fatty Acid Trafficking in Starved Cells: Regulation by Lipid Droplet Lipolysis, Autophagy, and Article Fatty Acid Trafficking in Starved Cells: Regulation by Lipid Droplet Lipolysis, Autophagy, and Mitochondrial Fusion Dynamics. *Dev. Cell* 32, 678–692. <https://doi.org/10.1016/j.devcel.2015.01.029>.
- Reggiori, F., Klionsky, D.J., 2013. Autophagic processes in yeast: Mechanism, machinery and regulation. *Genetics* 194, 341–361. <https://doi.org/10.1534/genetics.112.149013>.
- Ren, W., Zhang, Z., Shao, W., Yang, Y., Zhou, M., Chen, C., 2017. The autophagy-related gene BeATG1 is involved in fungal development and pathogenesis in *Botrytis cinerea*. *Mol. Plant Pathol* 18, 238–248. <https://doi.org/10.1111/mpp.12396>.
- Richie, D.L., Fuller, K.K., Fortwendel, J., Miley, M.D., McCarthy, J.W., Feldmesser, M., Rhodes, J.C., Askew, D.S., 2007. Unexpected link between metal ion deficiency and autophagy in *Aspergillus fumigatus*. *Eukaryot. Cell* 6 (12), 2437–2447.
- Rudd, J.J., Kanyuka, K., Hassani-Pak, K., Derbyshire, M., Andongabo, A., Devonshire, J., et al., 2015. Transcriptome and Metabolic Profiling of the Infection Cycle of *Zymoseptoria tritici* on Wheat Reveals a Biphasic Interaction with Plant Immunity Involving Differential Pathogen Chromosomal Contributions and a Variation on the Hemibiotrophic Lifest. *Plant Physiol.* 167, 1158–1185. <https://doi.org/10.1104/pp.114.255927>.

- Sánchez-Vallet, A., McDonald, M.C., Solomon, P.S., McDonald, B.A., 2015. Is *Zymoseptoria tritici* a hemibiotroph? *Fungal Genet. Biol.* 79, 29–32. <https://doi.org/10.1016/j.fgb.2015.04.001>.
- Shi, L., Wang, J., Quan, R., Yang, F., Shang, J., Chen, B., 2019. CpATG8, a homolog of yeast autophagy protein ATG8, is required for pathogenesis and hypovirus accumulation in the chest blight fungus. *Front. Cell. Infect. Microbiol.* 9, 1–8. <https://doi.org/10.3389/fcimb.2019.00222>.
- Shimamura, S., Miyazaki, T., Tashiro, M., Takazono, T., Saijo, T., Yamamoto, K., Imamura, Y., Izumikawa, K., Yanagihara, K., Kohno, S., Mukae, H., 2019. Autophagy-Inducing Factor Atg1 Is Required for Virulence in the Pathogenic Fungus *Candida glabrata*. *Front. Microbiol.* 10 <https://doi.org/10.3389/fmicb.2019.00027>.
- Shimizu, S., Kanaseki, T., Mizushima, N., Mizuta, T., Arakawa-Kobayashi, S., Thompson, C.B., et al., 2004. Role of Bcl-2 family proteins in a non-apoptotic programmed cell death dependent on autophagy genes. *Nat. Cell Biol.* 6, 1221–1228. <https://doi.org/10.1038/ncb1192>.
- Shoji, J.Y., Arioka, M., Kitamoto, K., 2006. Vacuolar membrane dynamics in the filamentous fungus *Aspergillus oryzae*. *Eukaryot. Cell* 5, 411–421. <https://doi.org/10.1128/EC.5.2.411-421.2006>.
- Shoji, J.Y., Craven, K.D., 2011. Autophagy in basal hyphal compartments: A green strategy of great recyclers. *Fungal Biol. Rev.* 25, 79–83. <https://doi.org/10.1016/j.fbr.2011.04.001>.
- Shoji, J.-y., Kikuma, T., Arioka, M., Kitamoto, K., Bassham, D., 2010. Macroautophagy-mediated degradation of whole nuclei in the filamentous fungus *Aspergillus oryzae*. *PLoS ONE* 5 (12), e15650.
- Sidhu, J.S., 2015. Molecular tools for functional genomic analyses of the stealth pathogenesis of wheat by *Zymoseptoria tritici*. University of Exeter. PhD Thesis.
- Sidhu, Y.S., Cairns, T.C., Chaudhari, Y.K., Usher, J., Talbot, N.J., Studholme, D.J., Csukai, M., Haynes, K., 2015. Exploitation of sulfonylurea resistance marker and non-homologous end joining mutants for functional analysis in *Zymoseptoria tritici*. *Fungal Genet. Biol.* 79, 102–109. <https://doi.org/10.1016/j.fgb.2015.04.015>.
- Singh, R., Kaushik, S., Wang, Y., Xiang, Y., Novak, I., Komatsu, M., Tanaka, K., Cuervo, A.M., Czaja, M.J., 2009. Autophagy regulates lipid metabolism. *Nature* 458 (7242), 1131–1135.
- Suffert, F., Delestre, G., Gélisse, S., 2019. Sexual Reproduction in the Fungal Foliar Pathogen *Zymoseptoria tritici* Is Driven by Antagonistic Density Dependence Mechanisms. *Microb. Ecol.* 77, 110–123. <https://doi.org/10.1007/s00248-018-1211-3>.
- Sumita, T., Izumitsu, K., Tanaka, C., 2017. Characterization of the autophagy-related gene BmATG8 in *Bipolaris maydis*. *Fungal Biology* 121, 785–797. <https://doi.org/10.1016/j.funbio.2017.05.008>.
- Suzuki, K., Kirisako, T., Kamada, Y., Mizushima, N., Noda, T., Ohsumi, Y., 2001. The pre-autophagosomal structure organized by concerted functions of APG genes is essential for autophagosome formation. *EMBO J.* 20, 5971–5981.
- Suzuki, K., Kubota, Y., Sekito, T., Ohsumi, Y., 2007. Hierarchy of Atg proteins in pre-autophagosomal structure organization. *Genes Cells* 12, 209–218. <https://doi.org/10.1111/j.1365-2443.2007.01050.x>.
- Tamura, N., Oku, M., Sakai, Y., 2010. Atg8 regulates vacuolar membrane dynamics in a lipidation-independent manner in *Pichia pastoris*. *J. Cell Sci.* 123, 4107–4116. <https://doi.org/10.1242/jcs.070045>.
- Torggler, R., Papinski, D., Kraft, C., 2017. Assays to Monitor Autophagy in *Saccharomyces cerevisiae*. *Cells* 6, 23. <https://doi.org/10.3390/cells6030023>.
- Torriani, S.F.F., Melichar, J.P.E., Mills, C., Pain, N., Sierotzki, H., Courbot, M., 2015. *Zymoseptoria tritici*: A major threat to wheat production, integrated approaches to control. *Fungal Genet. Biol.* 79, 8–12. <https://doi.org/10.1016/j.fgb.2015.04.010>.
- Veneault-Fourrey, C., Barooah, M., Egan, M., Wakley, G., Talbot, N.J., 2006. Autophagic Fungal Cell Death Is Necessary for Infection by the Rice Blast Fungus. *Science* 312, 580–583.
- Voigt, O., Pöggeler, S., 2013. Autophagy genes Smat8 and Smat4 are required for fruiting-body development, vegetative growth and ascospore germination in the filamentous ascomycete *Sordaria macrospora*. *Autophagy* 9, 33–49. <https://doi.org/10.4161/auto.22398>.
- Wang, Q., Liu, H., Xu, H., Hei, R., Zhang, S., Jiang, C., Xu, J.-R., 2019. Independent losses and duplications of autophagy-related genes in fungal tree of life. *Environ. Microbiol.* 21 (1), 226–243.
- Xie, Z., Klionsky, D.J., 2007. Autophagosome formation: Core machinery and adaptations. *Nat. Cell Biol.* 9, 1102–1109. <https://doi.org/10.1038/ncb1007-1102>.
- Yanagisawa, S., Kikuma, T., Kitamoto, K., 2013. Functional analysis of Aogat1 and detection of the Cvt pathway in *Aspergillus oryzae*. *FEMS Microbiol. Lett.* 338, 168–176. <https://doi.org/10.1111/1574-6968.12047>.
- Yemelin, A., Brauchler, A., Jacob, S., Laufer, J., Heck, L., Foster, A.J., Antelo, L., Andresen, K., Thines, E., Wilson, R.A., 2017. Identification of factors involved in dimorphism and pathogenicity of *Zymoseptoria tritici*. *PLoS ONE* 12 (8), e0183065.
- Ying, S.H., Liu, J., Chu, X.L., Xie, X.Q. & Feng, M.G. (2016) The autophagy-related genes BbATG1 and BbATG8 have different functions in differentiation, stress resistance and virulence of mycopathogen *Beauverria bassiana*. *Scientific Reports*, 6, 1–12. <https://doi.org/10.1038/srep26376>.
- Zhan, H., Yue, H., Zhao, X., Wang, M., Song, W., Nie, X., 2017. Genome-Wide Identification and Analysis of MAPK and MAPKK Gene Families in Bread Wheat (*Triticum aestivum* L.). *Genes* 8, 284. <https://doi.org/10.3390/genes8100284>.
- Zhang, Y., Qi, H., Taylor, R., Xu, W., Liu, L.F., Jin, S., 2007. The role of autophagy in mitochondria maintenance: Characterization of mitochondrial functions in autophagy-deficient *S. cerevisiae* strains. *Autophagy* 3, 337–346. <https://doi.org/10.4161/auto.4127>.
- van Zutphen, T., Todde, V., de Boer, R., Kreim, M., Hofbauer, H.F., Wolinski, H., Veenhuis, M., van der Klei, I.J., Kohlwein, S.D., Lemmon, S., 2014. Lipid droplet autophagy in the yeast *Saccharomyces cerevisiae*. *Mol. Biol. Cell* 25 (2), 290–301.
- Zwiers, L.H., De Waard, M.A., 2001. Efficient *Agrobacterium tumefaciens*-mediated gene disruption in the phytopathogen *Mycosphaerella graminicola*. *Curr. Genet.* 39 (5–6), 388–393. <https://doi.org/10.1007/s002940100216>.
- Goodwin, S. B., B. M'barek S, B. Dhillon, A. H. Wittenberg, C. F. Crane, J. K. Hane, A. J. Foster, T. A. Van der Lee, J. Grimwood, A. Aerts, J. Antoniw, A. Bailey, B. Bluhm, J. Bowler, J. Bristow, A. van der Burgt, B. Canto-Canché, A. C. Churchill, L. Conde-Ferràez, H. J. Cools, P. M. Coutinho, M. Csukai, P. Dehal, P. De Wit, B. Donzelli, H. C. van de Geest, R. C. van Ham, K. E. Hammond-Kosack, B. Henrissat, A. Kilian, A. K. Kobayashi, E. Koopmann, Y. Kourmpetis, A. Kuzniar, E. Lindquist, V. Lombard, C. Maliepaard, N. Martins, R. Mehrabi, J. P. Nap, A. Ponomarenko, J. J. Rudd, A. Salamov, J. Schmutz, H. J. Schouten, H. Shapiro, I. Stergiopoulos, S. F. Torriani, H. Tu, R. P. de Vries, C. Waalwijk, S. B. Ware, A. Wiebenga, L. H. Zwiers, R. P. Oliver, I. V. Grigoriev and G. H. Kema 2011. Finished genome of the fungal wheat pathogen *Mycosphaerella graminicola* reveals dispensome structure, chromosome plasticity, and stealth pathogenesis. *PLoS Genet.* 7, e1002070.